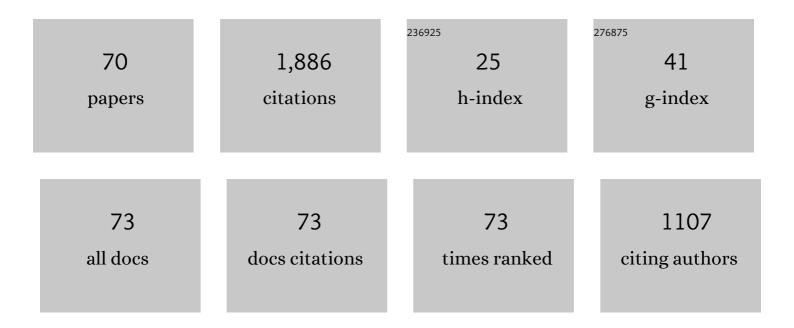
Hisao Takahashi

List of Publications by Year in descending order

Source: https://exaly.com/author-pdf/6627893/publications.pdf Version: 2024-02-01



Ηιςλο Τλκληλομι

#	Article	IF	CITATIONS
1	Magnetospheric disturbance induced equatorial plasma bubble development and dynamics: A case study in Brazilian sector. Journal of Geophysical Research, 2003, 108, .	3.3	152
2	Ionospheric plasma bubble climatology over Brazil based on 22 years (1977–1998) of airglow observations. Journal of Atmospheric and Solar-Terrestrial Physics, 2002, 64, 1517-1524.	1.6	131
3	Simultaneous observation of ionospheric plasma bubbles and mesospheric gravity waves during the SpreadFEx Campaign. Annales Geophysicae, 2009, 27, 1477-1487.	1.6	115
4	Gravity wave and tidal influences on equatorial spread F based on observations during the Spread F Experiment (SpreadFEx). Annales Geophysicae, 2008, 26, 3235-3252.	1.6	96
5	Convection: the likely source of the medium-scale gravity waves observed in the OH airglow layer near Brasilia, Brazil, during the SpreadFEx campaign. Annales Geophysicae, 2009, 27, 231-259.	1.6	79
6	An investigation of gravity wave activity in the low-latitude upper mesosphere: Propagation direction and wind filtering. Journal of Geophysical Research, 2003, 108, .	3.3	77
7	Characteristics of mesospheric gravity waves near the magnetic equator, Brazil, during the SpreadFEx campaign. Annales Geophysicae, 2009, 27, 461-472.	1.6	62
8	Ionospheric TEC Weather Map Over South America. Space Weather, 2016, 14, 937-949.	3.7	54
9	Overview and summary of the Spread F Experiment (SpreadFEx). Annales Geophysicae, 2009, 27, 2141-2155.	1.6	48
10	Equatorial plasma bubble seeding by MSTIDs in the ionosphere. Progress in Earth and Planetary Science, 2018, 5, .	3.0	48
11	Observations of day-to-day variability in precursor signatures to equatorial F-region plasma depletions. Annales Geophysicae, 1999, 17, 1053-1063.	1.6	44
12	The geospace response to variable inputs from the lower atmosphere: a review of the progress made by Task Group 4 of CAWSES-II. Progress in Earth and Planetary Science, 2015, 2, .	3.0	43
13	Plasma bubble monitoring by TEC map and 630nm airglow image. Journal of Atmospheric and Solar-Terrestrial Physics, 2015, 130-131, 151-158.	1.6	43
14	Periodic waves in the lower thermosphere observed by OI630â€⁻nm airglow images. Annales Geophysicae, 2016, 34, 293-301.	1.6	42
15	Comparison of gravity wave activity observed by airglow imaging at two different latitudes in Brazil. Journal of Atmospheric and Solar-Terrestrial Physics, 2004, 66, 647-654.	1.6	41
16	Reverse ray tracing of the mesospheric gravity waves observed at 23°S (Brazil) and 7°S (Indonesia) in airglow imagers. Journal of Atmospheric and Solar-Terrestrial Physics, 2006, 68, 163-181.	1.6	41
17	Plasma irregularities in the tropical Fâ€region detected by OI 7774 à and 6300 à nightglow measurements. Journal of Geophysical Research, 1981, 86, 3496-3500.	3.3	40
18	Evidence on 2-4 day oscillations of the equatorial ionosphere h′F and mesospheric airglow emissions. Geophysical Research Letters, 2005, 32, n/a-n/a.	4.0	38

HISAO TAKAHASHI

#	Article	IF	CITATIONS
19	Characteristics of equatorial plasma bubbles observed by TEC map based on ground-based GNSS receivers over South America. Annales Geophysicae, 2018, 36, 91-100.	1.6	38
20	Largeâ€scale traveling ionospheric disturbances observed by GPS dTEC maps over North and South America on Saint Patrick's Day storm in 2015. Journal of Geophysical Research: Space Physics, 2017, 122, 4755-4763.	2.4	37
21	Mediumâ€Scale Traveling Ionospheric Disturbances Observed by Detrended Total Electron Content Maps Over Brazil. Journal of Geophysical Research: Space Physics, 2018, 123, 2215-2227.	2.4	34
22	Mesospheric gravity waves observed near equatorial and low–middle latitude stations: wave characteristics and reverse ray tracing results. Annales Geophysicae, 2006, 24, 3229-3240.	1.6	32
23	Modeling the equatorial and lowâ€latitude ionospheric response to an intense Xâ€class solar flare. Journal of Geophysical Research: Space Physics, 2015, 120, 3021-3032.	2.4	30
24	16-day wave observed in the meteor winds at low latitudes in the southern hemisphere. Advances in Space Research, 2006, 38, 2615-2620.	2.6	27
25	Diagnostics of equatorial and low latitude ionosphere by TEC mapping over Brazil. Advances in Space Research, 2014, 54, 385-394.	2.6	27
26	Theoretical and experimental zonal drift velocities of the ionospheric plasma bubbles over the Brazilian region. Advances in Space Research, 2006, 38, 2610-2614.	2.6	26
27	Observation of mesospheric gravity waves at Comandante Ferraz Antarctica Station (62º S). Annales Geophysicae, 2009, 27, 2593-2598.	1.6	26
28	Investigation of Nighttime MSTIDS Observed by Optical Thermosphere Imagers at Low Latitudes: Morphology, Propagation Direction, and Wind Filtering. Journal of Geophysical Research: Space Physics, 2018, 123, 7843-7857.	2.4	25
29	Midnight reversal of ionospheric plasma bubble eastward velocity to westward velocity during geomagnetically quiettime: Climatology and its model validation. Journal of Atmospheric and Solar-Terrestrial Physics, 2011, 73, 1520-1528.	1.6	23
30	Rocket measurements of the equatorial airglow: MULTIFOT 92 database. Journal of Atmospheric and Solar-Terrestrial Physics, 1996, 58, 1943-1961.	0.9	22
31	Atomic oxygen concentrations from rocket airglow observations in the equatorial region. Journal of Atmospheric and Solar-Terrestrial Physics, 1996, 58, 1935-1942.	0.9	22
32	Mesospheric gravity waves and ionospheric plasma bubbles observed during the COPEX campaign. Journal of Atmospheric and Solar-Terrestrial Physics, 2011, 73, 1575-1580.	1.6	22
33	Possible influence of ultra-fast Kelvin wave on the equatorial ionosphere evening uplifting. Earth, Planets and Space, 2009, 61, 455-462.	2.5	21
34	Plasma bubble zonal drift characteristics observed by airglow images over Brazilian tropical region. Revista Brasileira De Geofisica, 2011, 29, 239-246.	0.2	20
35	Intrinsic parameters of periodic waves observed in the Ol6300 airglow layer over the Brazilian equatorial region. Annales Geophysicae, 2018, 36, 265-273.	1.6	16
36	Determinação dos parâmetros de ondas de gravidade através da análise espectral de imagens de aeroluminescência. Revista Brasileira De Geofisica, 2007, 25, .	0.2	14

HISAO TAKAHASHI

#	Article	IF	CITATIONS
37	Development of airglow temperature photometers with cooled-CCD detectors. Earth, Planets and Space, 2007, 59, 585-599.	2.5	13
38	Forward ray-tracing for medium-scale gravity waves observed during the COPEX campaign. Journal of Atmospheric and Solar-Terrestrial Physics, 2012, 90-91, 117-123.	1.6	12
39	Seasonal characteristics of small- and medium-scale gravity waves in the mesosphere and lower the Brazilian equatorial region. Annales Geophysicae, 2018, 36, 899-914.	1.6	11
40	Seasonal variation of plasma bubbles during solar cycle 23–24 over the Brazilian equatorial region. Advances in Space Research, 2019, 64, 1365-1374.	2.6	11
41	Equatorial Plasma Bubble Occurrence Under Propagation of MSTID and MLT Gravity Waves. Journal of Geophysical Research: Space Physics, 2020, 125, e2019JA027566.	2.4	10
42	An experimental study of the nightglow OH(8-3) band emission process in the equatorial mesosphere. Journal of Atmospheric and Solar-Terrestrial Physics, 1997, 59, 479-486.	1.6	9
43	Atmospheric wind effects on the gravity wave propagation observed at 22.7° S-Brazil. Advances in Space Research, 2003, 32, 819-824.	2.6	9
44	Comparison of the OH (8-3) and (6-2) band rotational temperature of the mesospheric airglow emissions. Revista Brasileira De Geofisica, 2004, 22, 223-231.	0.2	9
45	First observation of the diurnal and semidiurnal ocillation in the mesospheric winds over São João do Cariri-PB, Brazil. Revista Brasileira De Geofisica, 0, 25, .	0.2	9
46	The Prediction of Dayâ€ŧoâ€Đay Occurrence of Low Latitude Ionospheric Strong Scintillation Using Gradient Boosting Algorithm. Space Weather, 2021, 19, e2021SW002884.	3.7	9
47	The O2 Herzberg I bands in the equatorial nightglow. Journal of Atmospheric and Solar-Terrestrial Physics, 1997, 59, 295-303.	1.6	8
48	Atomic oxygen density profiles from ground-based nightglow measurements at 23°S. Journal of Geophysical Research, 2001, 106, 15377-15384.	3.3	8
49	Thermospheric F-region travelling disturbances detected at low latitude by an OI 630 nm digital imager system. Advances in Space Research, 2001, 27, 1201-1206.	2.6	8
50	Determination of gravity wave parameters in the airglow combining photometer and imager data. Annales Geophysicae, 2018, 36, 705-715.	1.6	8
51	Daytime ionospheric TEC weather study over Latin America. Journal of Geophysical Research: Space Physics, 2018, 123, 10,345.	2.4	8
52	Ultrafast Kelvin waves in the MLT airglow and wind, and their interaction with the atmospheric tides. Annales Geophysicae, 2018, 36, 231-241.	1.6	8
53	Case study of mesospheric front dissipation observed over the northeast of Brazil. Annales Geophysicae, 2018, 36, 311-319.	1.6	8
54	First results from mesospheric airglow observations at 7.5º S Revista Brasileira De Geofisica, 2001, 19, 169.	0.2	7

HISAO TAKAHASHI

#	Article	IF	CITATIONS
55	Planetary wave induced wind and airglow oscillations in the middle latitude MLT region. Journal of Atmospheric and Solar-Terrestrial Physics, 2013, 98, 97-104.	1.6	7
56	Lunar tides in total electron content over Brazil. Journal of Geophysical Research: Space Physics, 2017, 122, 7519-7529.	2.4	7
57	Atmospheric Gravity Waves Observed in the Nightglow Following the 21 August 2017 Total Solar Eclipse. Geophysical Research Letters, 2020, 47, e2020GL088924.	4.0	7
58	Climatology of equatorial and low-latitude F region kilometer-scale irregularities over the meridian circle around 120°E/60°W. GPS Solutions, 2021, 25, 1.	4.3	7
59	Why Do Equatorial Plasma Bubbles Bifurcate?. Journal of Geophysical Research: Space Physics, 2020, 125, e2020JA028609.	2.4	6
60	Asymmetric Development of Equatorial Plasma Bubbles Observed at Geomagnetically Conjugate Points Over the Brazilian Sector. Journal of Geophysical Research: Space Physics, 2022, 127, .	2.4	6
61	Effects of the planetary waves on the MLT airglow. Annales Geophysicae, 2017, 35, 1023-1032.	1.6	5
62	Long-Term Study on Medium-Scale Traveling lonospheric Disturbances Observed over the South American Equatorial Region. Atmosphere, 2021, 12, 1409.	2.3	5
63	Case Studies on Concentric Gravity Waves Source Using Lightning Flash Rate, Brightness Temperature and Backward Ray Tracing at São Martinho da Serra (29.44°S, 53.82°W). Journal of Geophysical Research D: Atmospheres, 2021, 126, e2020JD034527.	3.3	4
64	Semimonthly oscillation observed in the start times of equatorial plasma bubbles. Annales Geophysicae, 2020, 38, 437-443.	1.6	3
65	Nighttime Ionospheric TEC Study Over Latin America During Moderate and High Solar Activity. Journal of Geophysical Research: Space Physics, 2020, 125, e2020JA028210.	2.4	2
66	Disconnection and Reconnection in Plasma Bubbles Observed by OI 630Ânm Airglow Images From Cariri Observatory. Journal of Geophysical Research: Space Physics, 2022, 127, .	2.4	2
67	CARACTERISTICS OF IONOSPHERIC PLASMA BUBBLES OBSERVED BY TEC MAPS IN BRAZILIAN SECTOR. , 2017, , .		1
68	Influence of the semidiurnal lunar tide in the equatorial plasma bubble zonal drifts over Brazil. Annales Geophysicae, 2021, 39, 1005-1012.	1.6	1
69	Study of the gravity wave propagation direction observed by airglow imaging in the South American sector. , 2005, , .		0
70	Processamento de Dados de Rádio Ocultação da Constelação de Satélites COSMIC-2. , 2015, , .		0